(2)

OFFICE OF NAVAL RESEARCH

Contract N00014-82-K-0280

Task No. NR413E001

TECHNICAL REPORT NO. 31

The Adsorption and Thermal Decomposition of PH_3 on Si(111)-(7x7)

by

P.A. Taylor, R.M. Wallace, W.J. Choyke and J.T. Yates, Jr.

Prepared for Publication

in

Surface Science

Surface Science Center
Department of Chemistry
University of Pittsburgh
Pittsburgh, PA 15260

May 18 1990

SECURITY CLASSIFICATION OF THIS PAGE (When Data Entered)

REPORT DOCUMENTATION PAGE

READ INSTRUCTIONS BEFORE COMPLETING FORM

1. REPORT NUMBER: 31

2. GOVT ACCESSION NO.

3. RECIPIENT'S CATALOG NUMBER

4. TITLE (and Subtitle): The Adsorption and Thermal Decomposition of PH_3 on Si(111)-(7x7)

5. TYPE OF REPORT & PERIOD COVERED

6. PERFORMING ORG. REPORT NUMBER

7. AUTHOR(s): P.A. Taylor, R.M. Wallace, W.J. Choyke and J.T. Yates, Jr.

8. CONTRACT OR GRANT NUMBER(s)

9. PERFORMING ORGANIZATION NAME AND ADDRESS
Surface Science Center
Chemistry Department
University of Pittsburgh, Pittsburgh, PA 15213

10. PROGRAM ELEMENT, PROJECT, TASK AREA & WORK UNIT NUMBERS

11. CONTROLLING OFFICE NAME AND ADDRESS

12. REPORT DATE: 5-14-90

13. NUMBER OF PAGES: 40

14. MONITORING AGENCY NAME & ADDRESS (if different from Controlling Office)

15. SECURITY CLASS. (of this report)

15a. DECLASSIFICATION/DOWNGRADING SCHEDULE

16. DISTRIBUTION STATEMENT (of this Report)

17. DISTRIBUTION STATEMENT (of the abstract entered in Block 20, if different from Report)

18. SUPPLEMENTARY NOTES

19. KEY WORDS (Continue on reverse side if necessary and identify by block number)

Si(111)
PH_3
Phosphine
Phosphorus, Hydrogen Phosphide, Silicon, Surface Chemistry, Desorption, Dissociation, Doping (JG)

20. ABSTRACT: The adsorption of PH_3 on Si(111)-(7x7) has been studied by Auger electron spectroscopy and temperature programmed desorption. PH_3 was found to exhibit two kinds of behavior on the surface. A small surface coverage of molecularly adsorbed PH_3 desorbs without any dissociative surface chemistry. For the majority of the adsorbed PH_x species (3≥x≥1) dissociation occurs to form P(a) and H(a). At 120 K, PH_3 initially adsorbs as the reactive species with a sticking coefficient of S=1 up to ~75% saturation. The reactive PH_x species surface concentration saturates at $1.9\pm0.3\times10^{14}$ PH_x cm^{-2}. Surface H(a), produced by PH_x thermal decomposition, desorbs as H_2(g) at T>700 K, and P(a) desorbs as P_2(g) at T>900 K. Capping the Si-dangling bonds with atomic deuterium prevents PH_3 adsorption, indicating that the dangling bonds are the PH_3 adsorption sites. Isotopic studies involving Si-D surface species mixed with adsorbed PH_x species indicate that PH_3 desorption does not occur through a recombination process. Finally, additional PH_3 may be adsorbed if the surface hydrogen produced by dissociation of PH_3 is removed. Evidence for P penetration into bulk Si(111) at 875 K is presented.

DD FORM 1 JAN 73 1473 EDITION OF 1 NOV 65 IS OBSOLETE
S/N 0102-014-6601

SECURITY CLASSIFICATION OF THIS PAGE (When Data Entered)

Submitted to: Surface Science

Date: 14 May 1990

The Adsorption and Thermal Decomposition of PH_3 on Si(111)-(7x7)

P.A. Taylor, R.M. Wallace, W.J. Choyke and J.T. Yates, Jr.

Surface Science Center
Department of Chemistry
University of Pittsburgh
Pittsburgh, PA 15260

The Adsorption and Thermal Decomposition of PH_3 on Si(111)-(7x7)

P.A. Taylor, R.M. Wallace, W.J. Choyke and J.T. Yates, Jr.

Surface Science Center
Department of Chemistry
University of Pittsburgh
Pittsburgh, PA 15260

Abstract

The adsorption of PH_3 on Si(111)-(7x7) has been studied by Auger electron spectroscopy and temperature programmed desorption. PH_3 was found to exhibit two kinds of behavior on the surface. A small surface coverage of molecularly adsorbed PH_3 desorbs without any dissociative surface chemistry. For the majority of the adsorbed PH_x species ($3 \geq x \geq 1$) dissociation occurs to form P(a) and H(a). At 120 K, PH_3 initially adsorbs as the reactive species with a sticking coefficient of $S \approx 1$ up to ~75% saturation. The reactive PH_x species surface concentration saturates at $1.9 \pm 0.3 \times 10^{14}$ PH_x cm^{-2}. Surface H(a), produced by PH_x thermal decomposition, desorbs as $H_2(g)$ at T>700 K, and P(a) desorbs as $P_2(g)$ at T>900 K. Capping the Si-dangling bonds with atomic deuterium prevents PH_3 adsorption, indicating that the dangling bonds are the PH_3 adsorption sites. Isotopic studies involving Si-D surface species mixed with adsorbed PH_x species indicate that PH_3 desorption does not occur through a recombination process. Finally, additional PH_3 may be adsorbed if the surface hydrogen produced by dissociation of PH_3 is removed. Evidence for P penetration into bulk Si(111) at 875 K is presented.

I. Introduction

In the doping of silicon, phosphorus is often incorporated substitutionally to create a localized electron state below the conduction band. The phosphorus may be incorporated into the silicon lattice by either ion implantation of P^+ [1-4], or chemically using phosphorus-containing molecules added during the growth of silicon films [5-11]. The use of phosphine, PH_3, to dope films of a-Si:H with phosphorus during chemical vapor deposition (CVD) from silane has been shown to be effective [5-8; 10-12]. In these studies, however, a dramatic decrease in silicon deposition rate was observed, as compared to growth without phosphine, suggesting that species on the Si surface produced from PH_3 retard the surface decomposition of silane [5,6,10,12].

The adsorption of phosphine on Si(100) and its effects on the co-adsorption of silane has been studied by Yu and Meyerson [12]. They report that PH_3 "mostly adsorbs non-dissociatively" [13] with an initial sticking coefficient of $S_0 \approx 1.0$ at room temperature, compared to $S_0 = 0.0015$ for silane [12]. The adsorbed phosphine was reported to decompose at temperatures near 475 K into 3(Si-H) and Si-P [13]. At a temperature of 675 K, SIMS measurements indicate the desorption of surface hydrogen [12]. The desorption of hydrogen opens up silicon sites where further phosphine adsorption may take place. At temperatures above 875 K, surface phosphorus was depleted, as measured by Auger electron spectroscopy [12], leaving a clean silicon surface. Desorption of P_2 was later reported [13] in thermal desorption studies with an onset temperature of ~875 K and a peak maximum at ~975 K.

Van Bommel and Meyer [11] have reported a low energy electron diffraction (LEED) study of phosphine adsorption on Si(111) as a function of both surface temperature and phosphine pressure. The pressure vs temperature phase diagram

has seven different P-Si phases. The phosphine adsorbed at room temperature formed a P-(7x7) phase, stable to temperatures below 770 K, later shown to have 0.33 P/Si [14]. At a phosphine pressure of 10^{-7} Torr and a temperature of 770-790 K, a P-(1x1) phase is formed with H_2 desorption postulated, leading to a saturation surface coverage of 1 P/Si [14]. Further phosphine exposure (P $\sim 10^{-7}$ Torr) at temperatures of 800<T<900 K leads to a P-($6\sqrt{3}$x$6\sqrt{3}$) phase with a reported coverage of 3 P/Si [14]. At temperatures above 955 K the P-(1x1) phase returns, followed by a P-($2\sqrt{3}$x$\sqrt{3}$) phase with island formation (970-1020 K), followed by another P-(1x1) phase (1020-1070 K), and finally returning to a clean Si(111)-(7x7) crystal at temperatures above 1070 K.

In this work we show that phosphine adsorbs onto Si(111)-(7x7) with an initial sticking coefficient of S_0=1.0 at 120 K. Upon heating the adsorbed phosphine, hydrogen is removed from PH_x(a) ($3 \geq x \geq 1$) species to form Si-H bonds (T<700 K). Surface hydrogen then recombines to form H_2(g) (T>700 K), followed by surface phosphorus recombination to form P_2(g) (T>900 K). These results are qualitatively similar to those reported for PH_3 on Si(100) by Yu and Meyerson [12,13]. In addition, we show that: (1) Adsorbed PH_3 has two thermally activated reaction pathways which are coverage dependent. In the first pathway, molecularly chemisorbed PH_3 desorbs as PH_3(g). In the second pathway, the reactive species PH_x ($3 \geq x \geq 1$) thermally decompose into H(a) and P(a). (2) A direct observation of P(a) recombination to produce P_2(g) has been made. (3) P penetration into the near surface region occurs at 875 K.

In a separate paper we report additional studies of PH_3 adsorbed on Si(111)-(7x7), primarily employing electron stimulated desorption (ESD) methods [15].

II. Experimental

The experiments were carried out in a stainless steel ultra-high vacuum

(UHV) chamber with a base pressure of ~$3x10^{-11}$ Torr, shown schematically in Fig. 1. The UHV system is equipped with a Varian Scanning Auger electron spectrometer (AES), a low energy electron diffraction (LEED)/electron stimulated desorption ion angular distribution (ESDIAD) apparatus, a collimated gas doser [16], and two digitally multiplexed UTI-100C quadrupole mass spectrometers (QMS). Further details of the UHV system have been given elsewhere [15,17].

One of the quadrupole mass spectrometers is shielded from the random gas flux arriving at the ionization source. This shielded QMS (SQMS) has two apertures. The first aperture is a small circular aperture (diameter = 5.0 mm) which is on the quadrupole axis. The aperture is electrically isolated from the shield, and has an applied potential of -100 V to prevent irradiation of the silicon crystal by electron emission from the ionization source when the crystal is on the quadrupole axis (i.e. during thermal desorption studies). The second and larger aperture is rectangular (5.32 cm x 3.42 cm) and lies directly above the ionization cage. This aperture may be opened or closed in vacuum by a retractable door driven by a rack and pinion. When the door to the larger aperture is open, the SQMS primarily probes the random gas flux, which may be used to detect the rate of adsorption of a gas when the crystal is in front of the gas doser [18]. When closed, the SQMS primarily probes those gases which are traveling along the quadrupole axis and serves as a detector of thermal desorption from the center of the Si crystal when it is located in front of the aperture. Normally the crystal is located ~ 2 mm in front of the aperture. The SQMS is pumped by three circular holes (diameter = 1.1 cm) equally spaced on the lower rear circumference of the shield. More details on the SQMS are given in [15].

The phosphine studies were performed on a 1.30 x 1.31 x 0.15 cm Si(111) p-type, B-doped 10 ohm-cm single crystal, oriented to within 1° of the

(111) direction. The crystal was chemically cleaned [19], mounted [16], and finally rinsed with methanol prior to installation into the vacuum chamber. For final cleaning in ultra high vacuum the crystal was sputtered with 2keV Ar^+ at a crystal current of 2μA arriving at an incident angle of 70° with respect to the surface normal. After sputtering the crystal was subsequently annealed to 1175 K for 300-600 s, and slowly cooled to ~120 K (rate<5 K s^{-1}). This cleaning procedure produced a well-ordered Si(111)-(7x7) surface, as determined by LEED, free of surface impurities detectable by AES.

To calibrate the flux of PH_3 exiting the doser, the pressure drop in the gas handling system behind a nominal 2-micron conductance-limiting orifice was monitored over a period of 1.4×10^5 sec. A plot of $\ln\{P(t)/P(0)\}$ versus time, Fig. 2, gives a straight line with the slope, $-F/V$, equal to the leak rate of phosphine from the gas handling system through the orifice and into the UHV chamber, where F is the conductance of the orifice in molecules-cm^3 sec^{-1} and V is the volume behind the orifice ($V=209.2$ cm^3). From the slope in Fig. 2 we obtain a conductance of 5.94×10^{-4} cm^3 sec^{-1}, to give a flux exiting the doser of $F_{phosphine}=1.93 \pm 0.09 \times 10^{13}$ PH_3-molecules $Torr^{-1}$ sec^{-1}. The error reported for the flux is from a propagation of errors analysis.

The angular distribution of the phosphine effusing from the collimated doser is such that a portion of the flux misses the crystal. Campbell and Valone [20] and more recently Winkler and Yates [21] have shown that the flux intercepted by the crystal from a multicapillary-array collimator (diameter = 1.02 cm) can be determined from the known crystal-doser geometry. Using the method of Campbell and Valone [20] and a doser-crystal distance of 0.5 cm, we calculate that the fraction of the flux intercepted by a circular crystal of an area equal to our square crystal (d=1.474 cm) is $f_{cal}=0.70$. The fraction of the flux intercepted by the crystal can also be obtained experimentally [18].

Figure 3 shows an adsorption kinetics experiment for phosphine on Si(111)-(7x7) at 121 K, as monitored by measurements of the PH_3 signal using the SQMS with the large aperture door open (i.e. probing the random PH_3 flux resulting from the PH_3 flux which is not adsorbed by the crystal). In this experiment, the doser is turned on at 113 s with the crystal rotated away from the beam. Upon achievement of a stable PH_3 signal at 316 s, the clean Si(111) crystal is rotated into the PH_3 beam and an immediate drop in the scattered PH_3 signal is observed as adsorption of PH_3 occurs. The adsorption occurs at a constant rate until 415 s, when the rate of adsorption suddenly decreases and the scattered PH_3 flux rises slowly to a limiting value. We assume that the initial constant sticking coefficient for PH_3 is unity. With this assumption [18], the fractional interception of the PH_3 flux by the crystal, f_{exp}, may be measured as $\Delta_1/(\Delta_1+\Delta_2)$. From Fig. 3 we measure $f_{exp}=0.65$. From 14 separate experiments we obtain a mean fractional interception of $f_{exp}=0.64\pm0.07$ (1σ) in good agreement with the calculated result ($f_{cal}=0.70$) based on the geometry of the system, as described previously. Thus, the assumption of an initial sticking coefficient, $S_0\approx1$, is physically reasonable based on the agreement between the experimental measurements of the fraction intercepted and the predicted value ($f_{exp}\approx f_{calc}$). The constancy of the initial sticking coefficient over a large coverage range also supports its value of unity.

For temperature programmed desorption (TPD) studies, a modified digital temperature programmer [22] was used to heat the crystal at a reproducible rate of ~1.6 K sec^{-1} over the temperature range of 110 K to 1150 K. The SQMS was used in all the reported thermal desorption studies with the crystal reproducibly positioned ~2 mm in front of the smaller aperture and with the larger aperture closed. Both mass spectrometers were carefully calibrated for higher masses by leaking Kr into the UHV chamber.

The AES data reported herein represents the average of four measurements of the dN(E)/dE peak-to-peak heights taken at four points over the exposed area of the crystal. For Auger analysis, the electron gun typically delivered $2x10^{-6}$ A in a 0.2 mm diameter beam at the crystal. An extensive study of the P(LVV) lineshape and peak-to-peak amplitude showed no changes with prolonged electron beam exposure (up to 7.5 times the analysis time); therefore, the reported AES accurately measures the relative phosphorus surface coverage originating from strongly-bound PH_x ($3 \geq x \geq 1$) species which have been decomposed in the electron beam; the phosphorus surface coverage measurement should be considered as an assay of the strongly-bound PH_x species which are not desorbed by ESD. The reported phosphorus concentrations were calculated from the AES measurements using the appropriate elemental sensitivity factors [23].

III. Results

A. Adsorption of PH_3/Si(111).

The kinetics of adsorption of phosphine on Si(111)-(7x7) at 121 K can be observed as shown in Fig. 3. Once the crystal is rotated into the PH_3 flux, PH_3 adsorbs at a constant rate up to ~$1.6x10^{14}$ PH_3-molecules cm^{-2} (plateau region of constant rate of uptake). Eleven separate adsorption experiments gave a mean exposure value for the constant uptake region to be $1.5 \pm 0.2x10^{14}$ PH_3-molecules cm^{-2}. After the region of constant uptake, the PH_3 adsorption process becomes less efficient, indicating a decreasing sticking coefficient. The adsorption temperature throughout these adsorption experiments was T_{ads}=116±5 K.

Phosphine adsorption on Si(111)-(7x7) is further confirmed by the AES detection of surface phosphorus after the crystal is exposed to PH_3 (Fig. 4). On the basis of the Auger data in Fig. 4 where the increase of the phosphorus

coverage is measured versus PH_3 exposure, we estimate that about 70-75% of the PH_3 species detected by Auger spectroscopy adsorbs during the process with $S \approx 1$, and 25-30% during the process with $S<1$.

B. Desorption from PH_3/Si(111)

All the desorbing species observed from temperature programmed desorption of PH_3, adsorbed to saturation coverage on Si(111)-(7x7) at 120 K, are shown in Fig. 5. The thermal desorption data reveal two reaction pathways for adsorbed PH_3. In the first pathway, molecularly adsorbed PH_3 desorbs intact from the surface. In the second pathway, chemisorbed $PH_x(a)$ $(3 \geq x \geq 1)$ thermally decomposes to H(a) and P(a) species, which subsequently desorb as $H_2(g)$ and $P_2(g)$.

A thorough search for other desorbing species showed no other reaction products. Other products of primary concern were SiH_4 (m/e=32 and its fragment 30 (SiH_2^+)); Si_2H_6 fragment $Si_2H_5^+$ (m/e=61); SiP (m/e=59); P_2H_4 (m/e=66); and P_4 (m/e=124). In the case of SiH_3^+ and $Si_2H_6^+$ an interference occurs with P^+ and P_2^+ respectively; however, SiH_4 and Si_2H_6 may be eliminated as possible desorption products due to the lack of signal for their other known ionization fragments at 30 amu (SiH_2^+), 29 amu (SiH^+), 60 amu ($Si_2H_4^+$), and 58 amu ($Si_2H_2^+$) which do not coincide with the observed desorption species. No evidence for the desorption of any of these possible silane and disilane product species was found in these experiments.

The desorption of the molecular PH_3 does not occur if the PH_3 coverage is less than 1.5×10^{14} PH_3 cm^{-2}. This means that in the exposure region where $S \approx 1$ (Fig. 3), all of the adsorbed PH_3 will dissociate upon heating.

The desorption of the molecularly-bound PH_3 state as a function of PH_3 exposure is shown in Figs. 6 and 7. The molecular desorption of PH_3 exhibits a

desorption peak maximum at ~180 K with additional desorption processes extending to ~550 K. The large temperature range for PH_3 desorption in Fig. 6 suggests that several PH_3 chemisorption states are responsible for the molecular desorption of PH_3. From Fig. 7 one can clearly see that the molecularly adsorbed PH_3 state, measured by thermal desorption, does not saturate until PH_3 exposures greater than ~35×10^{14} PH_3 cm^{-2} have occurred; however the data in Fig. 4 shows that the phosphorus surface concentration as measured by Auger spectroscopy saturates at an exposure of ~5×10^{14} PH_3 cm^{-2}. The lack of increase in the P Auger intensity beyond a PH_3 exposure of ~5×10^{14} PH_3 cm^{-2} suggests that the coverage of molecular PH_3 responsible for PH_3 desorption is small. This idea is verified in Fig. 5 by comparing the integrated thermal desorption yield of $PH_3(g)$ to that of $H_2(g)$. Note that mass spectrometer sensitivity for $H_2(g)$ is 10^{-2} compared to that for $PH_3(g)$. The small relative yield of PH_3 compared to H_2 (coming from dissociation of PH_3) suggests that only a small coverage of PH_3 which desorbs as molecular PH_3 is present even after an exposure of ~35×10^{14} PH_3 cm^{-2}.

Figure 8 shows the thermal desorption behavior of P_2 from Si(111) exposed to PH_3. The desorption of phosphorus exclusively as $P_2(g)$ is expected at the low pressures of the TPD experiments, where considerations of equilibrium would strongly favor P_2 production. This was confirmed experimentally where both P_4^+ (m/e=124 amu) and P_3^+ (m/e=93 amu) were shown to be absent (see ref. 25 and 26 for P_4 cracking pattern information).

The ionization cracking pattern of $P_2(g)$ has been obtained by heating InP or GaP to temperatures above 870 K [27,28]. The ionization of $P_2(g)$ with 70 eV electrons is reported to give a fragmentation pattern of P_2^+:P^+ in the ratio of 100:12, respectively [28]. From the inset in Fig. 8, the ratio of the desorption yields of P_2^+ and P^+ from Si(111) is approximately 100:67. Despite

the difference in cracking patterns between the literature [28] and the work reported here, the agreement in the desorption peak shapes for P_2 and P strongly suggests that the two species are related, and that P^+ is a mass-spectrometer cracking product of P_2. The symmetric shape of the P_2 desorption features (Fig. 8), and the T_{max} shift towards lower temperatures with increasing initial coverage, suggest that P_2 desorbs with second order-kinetics. Using second order kinetics, the activation energy of desorption for P_2 from P/Si(111) at the zero coverage limit was estimated to be $E_d \cong 87$ kcal mole^{-1}, using the method of Chan, Aris and Weinberg [29] and the second-order pre-exponential factor at the zero coverage limit was estimated to be $\nu_d = 10^{2\pm1}$ cm^2 sec^{-1}. To calculate the pre-exponential factor we assumed that all 19 dangling bonds in the Si(111)-(7x7) cell [30] are reactive and there is 1P/Si-dangling bond on a fully-covered surface. Arguments to be presented later suggest that a P coverage of 1P/Si-dangling bond is possible sterically when PH_3 is the adsorbate. However, this assumption may not be strictly accurate, considering that different reactivity of the Si(111)-(7x7) dangling bonds may exist, as has been observed for NH_3 on Si(111) [31].

A major desorption product shown in Fig. 5 is molecular hydrogen. This desorption process corresponds closely to that observed when atomic H is adsorbed on Si(111) in the monohydride adsorption state [32], as will be shown below.

C. Si(111) Site Blocking by Deuterium.

It is well-known that the pre-adsorption of atomic deuterium (or hydrogen) onto silicon will cap the surface dangling bonds and reduce the adsorptive capacity of the surface. This effect has been observed for the NH_3/D/Si(100) system [17] and for the adsorption of unsaturated hydrocarbons on Si(100) [33].

Similar results are observed for the PH_3/D/Si(111)-(7x7) system, demonstrating that the dangling bonds are the active sites for phosphine adsorption.

The atomic deuterium is produced by the dissociation of D_2(g) on a tungsten filament at 1800 K [17]. The atomic D exposures are reported in Langmuirs (L) of D_2(g) exposed to the W-filament, where 1 L=1×10^{-6} Torr-sec (uncorrected for ion gauge sensitivity to D_2). The well-known β_1-monodeuteride and β_2-dideuteride desorption states develop on Si(111) with increasing exposure to atomic D, as shown in Fig. 9. To calibrate the D(a) coverage, the onset of the surface dideuteride production (5 L D_2), as observed by the desorption of the well-known β_2-D_2 state, was taken as an index of monolayer D(a) coverage, as shown in the inset of Fig. 9. This is an arbitrary criterion of the monolayer capacity for D, and it is observed from the data in Fig. 9 that the β_1 (monodeuteride) desorption yield continues to increase above this arbitrarily-defined monolayer point.

The effect of pre-adsorbed deuterium on the PH_3 adsorption kinetics is to decrease the amount of adsorbed PH_x. The decrease in the amount of PH_x adsorbed, with increasing D(a) coverage, is indicated by the drop in the surface phosphorus concentration as measured by AES (Fig. 10) for a saturation PH_3 exposure on the D-capped Si(111) surface. The surface is passivated by a 7-L D_2 exposure which is near the onset of the β_2-dideuteride production, as shown in Fig. 9 for the D atom experiments.

A search for deuterium-labelled phosphine desorption products, shown in Fig. 11, clearly indicate that no isotope exchange processes occur on the Si(111) surface between molecularly adsorbed PH_3 and D(a). This result indicates that recombination of a PH_x(a) species with H(a) is not responsible for either the sharp PH_3 desorption feature (T~180 K) or for the PH_3 desorption processes up to ~550 K (as seen in Figs. 5 and 6).

For atomic D coverages yielding the β_2 (dideuteride) desorption state, etching of the Si surface was observed as indicated by the desorption product SiD_4. This result agrees with the observed etching of silicon surfaces by hydrogen recently reported by Greenlief et al. [34].

D. Phosphine Adsorption on P/Si(111).

A saturated, phosphine-covered Si(111) surface may adsorb additional PH_3 if the pre-adsorbed PH_3 is heated sufficiently to remove the adsorbed hydrogen. In Fig. 12 the P(LVV) AES peak-to-peak intensity is reported for experiments involving PH_3 exposure followed by heating to two different temperatures, followed by a re-exposure to PH_3 at 115 K. In the first thermal treatment, the saturated PH_3 layer (exposure= ϵ_1) was heated to below the onset of the H_2 desorption (615 K), as indicated by the dashed arrow in Fig. 12, and re-exposed to another saturation exposure of PH_3, ϵ_2. A slight increase in the P(LVV) peak-to-peak intensity after the second exposure indicates that only a very small additional adsorption of PH_3 can take place on the PH_3 pre-covered surface which still contains adsorbed hydrogen produced by PH_3 thermal decomposition. In the second experiment the surface containing the saturated PH_3 exposure, as produced by ϵ_1, was heated to 875 K, which is <u>beyond</u> the H_2 desorption temperature but <u>prior to</u> the P_2 desorption temperature. The crystal was then re-exposed to a second saturation exposure of PH_3, ϵ_2. In the second exposure, the kinetic uptake curve was identical to that shown in Fig. 3 (not shown), and the P(LVV) peak-to-peak intensity doubles over that of the first exposure (Fig. 12). This behavior indicates a regeneration of PH_3 adsorption sites on the Si(111) surface upon desorption of hydrogen.

The Si(111) surface has a large capacity for the adsorption of phosphorus. The exposure-anneal-exposure cycle, described above, can be repeated several

times without a significant attenuation in the Si(111) adsorption capacity for PH_3, as shown by the increase of the P(LVV) AES peak-to-peak intensity with incremental PH_3 exposures in Fig. 13. A change in the surface structure between the clean Si(111)-(7x7) structure and the P/Si(111)-(1x1) structure after ϵ_5 was also observed by LEED (not shown), in agreement with the work of van Bommel et al. [11].

A small increase in the P(LVV) peak-to-peak intensity also occurs when the PH_3-covered surface is heated to cause removal of surface hydrogen. This small, although reproducible, increase in P(LVV) peak-to-peak intensity is due to the thermal loss of P-H bonds that slightly affects the P(LVV) lineshape and slightly increases the measured peak-to-peak intensity. Further details of the effects of hydrogen on the P(LVV) and Si(LVV) AES signals are given in another paper [15].

Studies of the behavior of the Si(LVV) Auger intensity were also carried out during the PH_3 exposure-anneal-exposure cycles. The increase in the atomic fraction of P upon sequential adsorption-anneal cycles is accompanied by a concomitant decrease in the Si(LVV) AES intensity as shown in Fig. 14.

IV. Discussion.

A. Saturation Coverage PH_3/Si(111) at 120 K.

The adsorption of PH_3 on Si(111)-(7x7) occurs at 120 K at a constant rate corresponding to unit adsorption efficiency up to $1.5\pm0.2\times10^{14}$ PH_3-molecules cm^{-2}. If we assume that PH_3 adsorbed during the $S\approx1$ process is the primary source of reactive PH_x, which ultimately forms surface phosphorus, then an estimate of the PH_x saturation coverage can be made. From the measured PH_x coverage at the end of the $S\approx1$ process and the additional phosphorus uptake,

measured by AES, during the S<1 process (see Fig. 4), the PH_x species saturation coverage, produced from PH_3, is calculated to be $1.9\pm0.3\times10^{14}$ PH_x cm^{-2} at 120 K.

From STM measurements the ideal Si(111)-(7x7) surface has 19 dangling bonds, (d-b), or reactive sites per unit cell [31], which corresponds to 3.0×10^{14} Si d-b cm^{-2}. Therefore, the PH_x species saturation coverage can also be expressed as θ_{sat}=0.5-0.7 PH_x/Si-dangling bond.

The assumption of equal participation of all 19 dangling bonds in the unit cell may not be accurate. Different reactivity of the Si(111)-(7x7) dangling bonds has been observed for NH_3 on Si(111) [31]. For ammonia on Si(111)-(7x7) the rest-atoms were found to be most reactive (6 d-b) followed by the adatoms (12 d-b). The center-adatoms in the (7x7) unit cell also were found to be more reactive to NH_3 than corner-adatoms in a ratio of reactivity of ~2:1. The reactivity towards NH_3 was not reported for the Si-dangling bonds in the holes at the corners of the (7x7) cell; therefore, we assume that the Si-dangling bonds in the holes at the corners of the (7x7) cell are non-reactive. If PH_3 adsorbs on Si(111) as NH_3 does, then there would be 15 dangling bonds per unit cell (6 rest-atoms + 6 center-adatoms + 3 corner-adatoms = 15 d-b/unit cell). For this type of bonding scheme the PH_x saturation coverage would be ~0.7-0.9 PH_x/Si-dangling bond.

B. Adsorption Kinetics - PH_3/Si(111)

The kinetics of adsorption of PH_3 on Si(111)-(7x7) at 120 K show clearly that the initial sticking coefficient is unity, and that it remains constant for a coverage extending up to ~75% of the saturation coverage for chemisorbed PH_x species. The large range of coverages which exhibits constant sticking coefficient kinetics clearly indicates that adsorption occurs via an extrinsic mobile precursor state, and that the lifetime of the pecursor is long enough for

migration to occur over filled states to empty adsorption sites.

The end of the S≈1 adsorption process in Fig. 3 is marked by an abrupt transition between S≈1 and S<1. It is worthwhile to speculate as to the nature of this transition. One possibility is that adsorbed PH_x sterically blocks incoming PH_3 molecules, decreasing the adsorption probability (S<1). A test of such a model is to "pack" PH_3 into the Si(111)-(7x7) cell (6.27×10^{-14} cm^2) using the van der Waals radii for PH_3 (r=1.72 Å [35]). A cubic packing of PH_3 would produce ~53 PH_3/Si-unit cell and close-packing (hcp) would produce ~61 PH_3/Si-unit cell. Both of these packing arrangements sterically allow considerably more than 1 PH_3/dangling bond. Therefore, we must conclude that steric blocking arguments cannot account for the abrupt change in the kinetics of the adsorption process. Another possibility is that PH_3 adsorbs predominantly dissociatively as PH_x ($2 \geq x \geq 1$) in the S≈1 region [13,15]. The PH_3 coverage at the end of the constant uptake region (S≈1) is 9 PH_3/Si-unit cell (1.6×10^{14} PH_3 cm^{-2}) consistent with a model where PH_3 may adsorb dissociatively in the S≈1 region primarily as PH_2(a) and H(a), with PH_2(a) and H(a) together occupying 15-19 dangling bond sites. If PH_3 dissociatively adsorbs initially as PH_2(a) + H(a), then both PH_3 and NH_3 adsorb on Si(111)-(7x7) in the same manner [31,36].

C. Adsorption Kinetics for PH_3/D/Si(111).

Blocking the Si(111) dangling bond sites by pre-adsorbed D atoms prevents PH_3 adsorption. This is observed by a reduction in the surface phosphorus concentration achieved by PH_3 adsorption on Si(111) containing increasing deuterium coverages. These results indicate that the Si-dangling bonds are the adsorption sites for PH_3 on Si(111)-(7x7). To within the accuracy of our measurements, it may be concluded that a saturated monodeuteride coverage is

sufficient to block PH_3 adsorption on Si(111)-(7x7).

D. Thermal Desorption from PH_3/Si(111)

The thermal desorption results indicate that adsorbed phosphine has two reaction pathways. In the first pathway, molecularly adsorbed PH_3 desorbs as PH_3(g), with no observable surface chemistry. In the second pathway, adsorbed PH_x decomposes into P(a) and H(a), which eventually desorbs as H_2(g) (T>700 K) and P_2(g) (T>900 K). The desorption of P_2(g) has been reported from PH_3 decomposition on Si(100) [13]. Further details of the thermal decomposition of PH_x adsorbed on Si(111)-(7x7) are given elsewhere [15].

E. Phosphine adsorption on P/Si(111)

If an adsorbed layer of PH_3 is heated beyond the hydrogen desorption temperature and below the phosphorus desorption temperature (T~875 K), then additional PH_3 may be adsorbed onto the P/Si(111) layer. This process may be repeated several times before saturation occurs, showing the large capacity of Si(111) for adsorption of phosphorus.

As the P(LVV) peak-to-peak intensity increases with the incremental PH_3 exposures (Fig. 13), the Si(LVV) peak-to-peak intensity decreases, as shown in Fig. 14. The attenuation of the Si(LVV) peak-to-peak intensity is caused by P screening of Si atoms. A simple estimate of the thickness of the adsorbed phosphorus after ϵ_5 may be obtained from the observed attenuation of the Si(LVV) AES intensity by using the expression $d = \lambda \ln(I_0/I)$, where d is the thickness of the phosphorus layer, λ is the escape depth of the Si(LVV) Auger electron through a phosphorus layer ($\lambda \approx$ 5Å [37]), and I_0 is the initial Si(LVV) intensity. Based on this expression, the calculated value of d≈ 1 Å. This is equivalent to a P coverage of $3.6\text{-}5.2 \times 10^{14}$ P cm^{-2} depending on the density

($g\ cm^{-3}$) assumed for overlayers of P.

The distribution in depth of the surface phosphorus may be inferred from the P coverage causing the observed screening of the Si AES signal. We assume from our quantitative uptake measurements that the PH_x coverage (following ϵ_1)=$1.9\pm0.3\times10^{14}$ PH_x cm^{-2} corresponding to a P(LVV) AES intensity of 1.6 arbitrary units (no heating, Fig. 12). After 5 cycles of PH_3 adsorption to ϵ_5, the P(LVV) AES intensity has increased to 7.8 arbitrary units. If all of this P was on the surface, the coverage would be $9.3\pm1.5\times10^{14}$ P cm^{-2}. If penetration of some of the P has occurred as a result of the successive annealing cycles, the number of P atoms cm^{-2} would exceed $9.3\pm1.5\times10^{14}$ P cm^{-2}. Thus, the attenuation of the Si(LVV) Auger intensity by P corresponds to a considerably lower surface coverage of P ($3.6-5.2\times10^{14}$ P cm^{-2}) than is measured from the P(LVV) intensity calibrated against a quantitative PH_3 uptake measurement. This implies that substantial P penetration into the near surface region of Si(111) has occurred upon annealing to 875 K. This subsurface P can be liberated as $P_2(g)$ on heating as shown in Fig. 8.

V. Summary

The behavior of phosphine on Si(111)-(7x7) studied by AES and TPD may be summarized as follows:

1. Phosphine adsorbs onto Si(111)-(7x7) at 120 K into a reactive PH_x ($3\geq x\geq1$) species with a sticking coefficient of $S\approx1$ up to ~75% of the PH_x saturation coverage.
2. The saturation coverage of reactive phosphine species on Si(111) is approximately 0.5-0.7 PH_x/Si-dangling bond (assuming 19 dangling bonds per Si(111)-(7x7) unit cell).

3. At coverages greater than ~1.5×10^{14} PH_3 cm^{-2}, a molecularly-bound PH_3 state exists which does not lead to any thermally-induced surface chemistry. This $PH_3(a)$ species is present at a coverage corresponding to a small fraction of a monolayer.
4. Surface Si-H species formed by PH_x thermal decomposition recombine to desorb as $H_2(g)$ at $T \geq 700$ K, and surface Si-P bonds break to yield $P_2(g)$ at $T \geq 900$ K. The kinetic parameters for second order desorption of $P_2(g)$ are $\nu_d = 10^{2\pm1}$ cm^2 sec^{-1} and $E_d \cong 87$ kcal $mole^{-1}$.
5. Phosphine may be used as a source for the continued deposition of surface phosphorus, after removal of surface hydrogen. Phosphorus penetration into the bulk occurs to some degree following heating to 875 K.

6. Acknowledgements

The full support of this work by the Office of Naval Research (ONR) is gratefully acknowledged. The authors would also like to thank Ms. Shenda Baker for her contributions in the exploratory stage of the experiments.

References

1. R.B. Fair, J. Vac. Sci. Technol., A4 (1986) 926.
2. G.S. Oehrlein, S.A. Cohen and T.O. Sedgwick, Appl. Phys. Lett. 45 (1984) 417.
3. F.F. Morehead and R.T. Hodgson, in Proceedings of the Material Research Society Symposium, D.K. Biegelsen, G.A. Rozgonyi and C.V. Shank (editors), Pittsburgh, Pa 1985 p. 341.
4. M.M. Mandurah, K.C. Saraswat, C.R. Helms and T.I. Kamins, J. Appl. Phys. 51 (1980) 5755.
5. B.S. Meyerson and W. Olbricht, J. Electrochem. Soc., 131 (1984) 2361.
6. B.S. Meyerson and M.L. Yu, J. Electrochem. Soc., 131 (1984) 2366.
7. B.S. Meyerson, B.A. Scott and D.J. Wolford, J. Appl. Phys. 54 (1983) 1461.
8. H. Kurokawa, J. Electrochem. Soc., 129 (1982) 2620.
9. T.I. Kamins, J. Electrochem. Soc., 126 (1979) 833.
10. F.C. Eversteyn and B.H. Pot, J. Electrochem. Soc., 120 (1973) 106.
11. A.J. van Bommel and F. Meyer, Sur. Sci. 8 (1967) 381.
12. M.L. Yu and B.S. Meyerson, J. Vac. Sci. Technol. A2 (1984) 446.
13. M.L. Yu, D.J. Vitkavage and B.S. Meyerson, J. Appl. Phys., 59 (1986) 4032.
14. A.J. van Bommel and J.E. Crobeen, Sur. Sci. 36 (1973) 773.
15. R.M. Wallace, P.A. Taylor and J.T. Yates, Jr., submitted to J. Appl. Phys.
16. M.J. Bozack, L. Muehlhoff, J.N. Russell, Jr., W.J. Choyke and J.T. Yates, Jr., J. Vac. Sci. Technol. A5 (1987) 1.
17. M.J. Dresser, P.A. Taylor, R.M. Wallace, W.J. Choyke and J.T. Yates, Jr., Sur. Sci. 218 (1989) 75.
18. V.S. Smentkowski and J.T. Yates, Jr., J. Vac. Sci. Technol. A7 (1989) 3325.
19. F. Bozso, J.T. Yates, Jr., W.J. Choyke and L. Muehlhoff, J. Appl. Phys. 57 (1985) 2771.

20. C.T. Campbell and S.M. Valone, J. Vac. Sci. Technol. A3 (1985) 408.

21. A. Winkler and J.T. Yates, Jr., J. Vac. Sci. Technol. A6 (1988) 2929.

22. P.A. Taylor, R.M. Wallace, C.-C. Cheng, W.H. Weinberg, M.J. Dresser, W.J. Choyke and J.T. Yates, Jr., to be submitted to Sur. Sci.

23. L.E. Davis, N.C. MacDonald, P.W. Palmberg, G.E. Riach and R.E. Weber, "Handbook of Auger Electron Spectroscopy," Perkin-Elmer, Eden Prairie, MN 1978.

24. D.E.C. Corbridge, "The Structural Chemistry of Phosphorus," Elsevier Scientific Publishing Company, New York, 1974, p. 14.

25. L. Kerwin, Canadian J. Phys. 32 (1954) 757.

26. J.S. Kane and J.H. Reynolds, J. Chem. Phys. 25 (1956) 342.

27. J.R. Arthur in "The Structure and Chemistry of Solid Surfaces," Proceeding of the Fourth International Materials Symposium, Berkeley, CA 1968, G. Somorjai (editor), Wiley, New York, 1969, p. 46-1.

28. J. Drowart and P. Goldfinger, J. Chim. Phys. 55 (1958) 721.

29. C.M. Chan, R. Aris, W.H. Weinberg, Appl. Sur. Sci. 1 (1978) 360.

30. R.M. Tromp, R.J. Hamers and J.E. Demuth, Phys. Rev. (1986) 1388.

31. R. Wolkow and Ph. Avouris, Phys. Rev. Lett. 60 (1988) 1049.

32. G. Schulze and M. Henzler, Sur. Sci. 124 (1983) 336.

33. M.J. Bozack, W.J. Choyke, L. Muehlhoff and J.T. Yates, Jr., Sur. Sci. 176 (1986) 547.

34. C.M. Greenlief, S.M. Gates and P.A. Holbert, Chem. Phys. Lett. 159 (1989) 202.

35. Handbook of Chemistry and Physics, 63rd Edition, Ed. R.C. Weast, CRC Press, Boca Raton, FL, 1982-1983, p. D-195.

36. S. Tanaka, M. Onchi and M. Nishijima, Sur. Sci. 191 (1987) L756.

37. C.J. Powell, private communication. Here it is assumed that $\lambda_p = \lambda_{Si} = 5$ Å at 92 eV.

Figure Captions

Figure 1. Schematic of the UHV chamber used in these studies.

Figure 2. Calibration of the PH_3 flux from the doser.

Figure 3. Adsorption kinetics for PH_3 on Si(111)-(7x7) at 121 K. Flux of PH_3 at the crystal = 1.6×10^{12} PH_3 molecules cm^{-2} sec^{-1}. $P_0(PH_3)$=0.214 Torr. The PH_3 pressure "spike" at t=1512 s is due to mechanical shock to the cooling coils which have adsorbed PH_3 from the background gas.

Figure 4. The surface concentration of phosphorus with increasing PH_3 exposure as probed by AES. Error bars represent 1σ deviation from the average of 4 AES measurements taken over the crystal area. The ordinate represents the atomic fraction of P in the depth of Auger sampling.

Figure 5. Thermal desorption spectra of all the desorbing species observed from PH_3/Si(111)-(7x7). The temperature ramp used in these studies was dT/dt= 1.6 K sec^{-1}. Comparison of the integrated area of the PH_3 to that of H_2 suggest that the observed PH_3(g) corresponds only to a small fraction of a monolayer.

Figure 6. Thermal desorption of molecular PH_3 from the molecularly-bound PH_3 surface state on Si(111).

Figure 7. Integrated TPD yield of molecular PH_3 as a function of surface exposure to PH_3 for the TPD curves shown in Fig. 6. Note: saturation occurs at PH_3 exposures greater than $\sim 35 \times 10^{14}$ PH_3 cm^{-2}.

Figure 8. Thermal desorption yield of P_2 as a function of PH_3 exposure. Inset shows the P_2^+ and P^+ mass spectrometer traces. The PH_3 exposures ($x10^{14}$ PH_3 cm^{-2}) are a: 0.7, b: 1.4, and c: 6.9 (saturated). The linear heating rate through the P_2 desorption features was dT/dt= 1.5 K s^{-1}.

Figure 9. Deuterium coverage calibration for phosphine-deuterium co-adsorption studies. D_2 exposures are reported in Langmuirs of D_2. The onset of the dihydride production as observed by TPD is arbitrarily defined as 1 monolayer D coverage (~5L D_2 in this case).

Figure 10. The effect capping the Si-dangling bonds, with atomic deuterium, on the adsorption of PH_3 measured by Auger spectroscopy. PH_3 exposure= $2.7x10^{14}$ PH_3 cm^{-2} at 130 K.

Figure 11. Thermal desorption from PH_3 co-adsorbed on a partially capped D/Si(111)-(7x7) surface. No isotope mixing to produce deuterated phosphine species is observed. D_2 exposure= 3 L; PH_3 exposure= $3.0x10^{14}$ cm^{-2}.

Figure 12. The re-adsorption capacity of an exposed PH_3/Si(111) surface after annealing to 615 K or to 875 K. Incremental exposures are $17.4x10^{14}$ PH_3 cm^{-2}, a saturation exposure.

Figure 13. The addition of surface phosphorus by repetitive exposure-anneal-exposure cycles of PH_3 on Si(111) as probed by the P(LVV) AES signal. The adsorption temperature was 115 K and the subsequent annealing temperature was 875 K. P_2 does not desorb at 875 K.

Figure 14. The attenuation of the Si(LVV) AES signal during the exposure-anneal-exposure cycles of PH_3 on Si(111). Adsorption temperature was 115 K and annealing temperature was 875 K. See Fig. 13.

Ultrahigh Vacuum Apparatus for Silicon Surface Chemistry

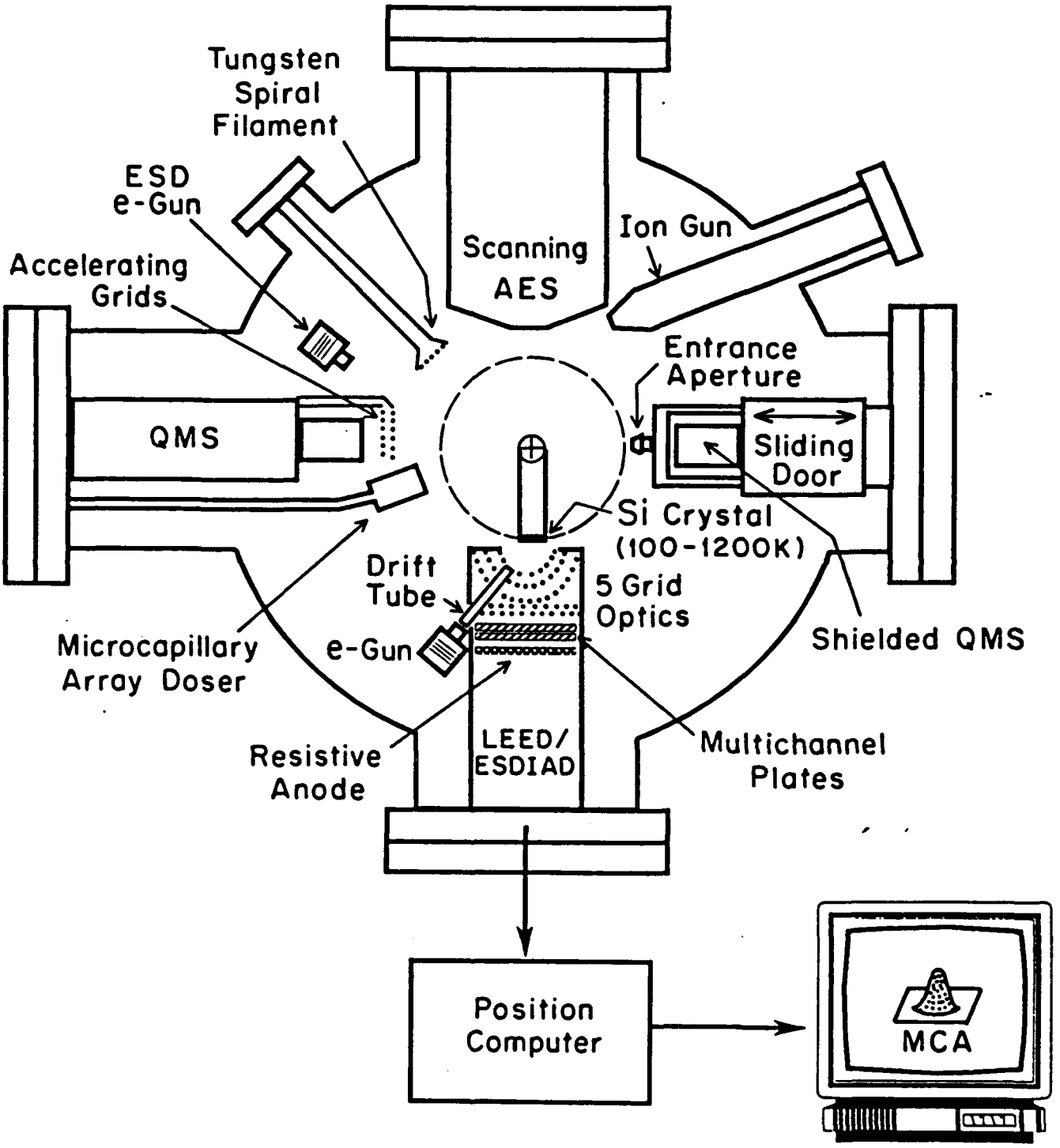

Taylor,
Wallace,
Choyke, Yat
Figure 1

Taylor,
Wallace,
Choyke, Yates
Figure 2

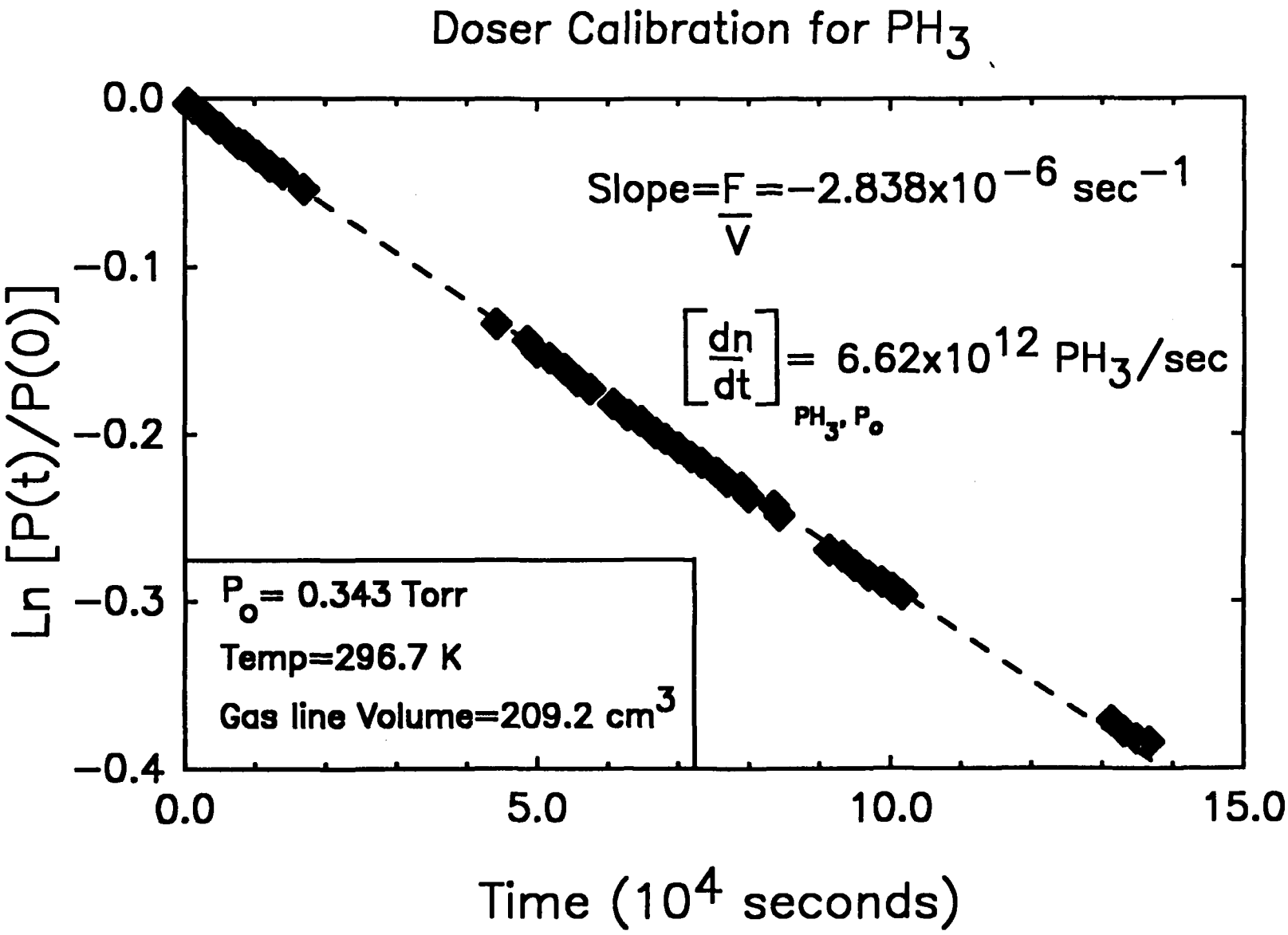

Taylor,
Wallace,
Choyke, Yate
Figure 3

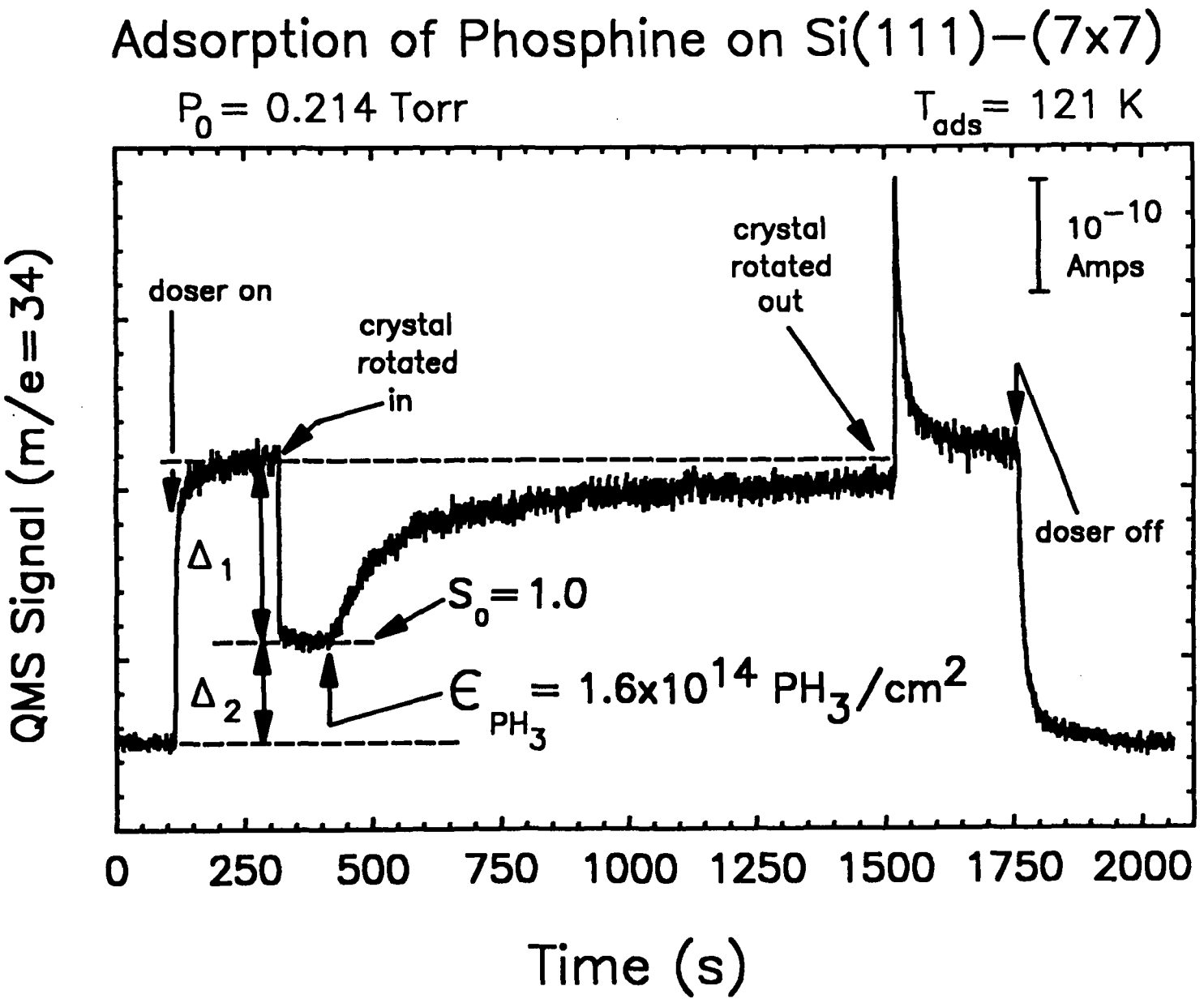

Taylor, Wallace, Choyke, Yates, Figure 7

AES Measurements of Phosphorus Surface Concentration with increasing PH_3 exposure. Si(111)–(7x7)

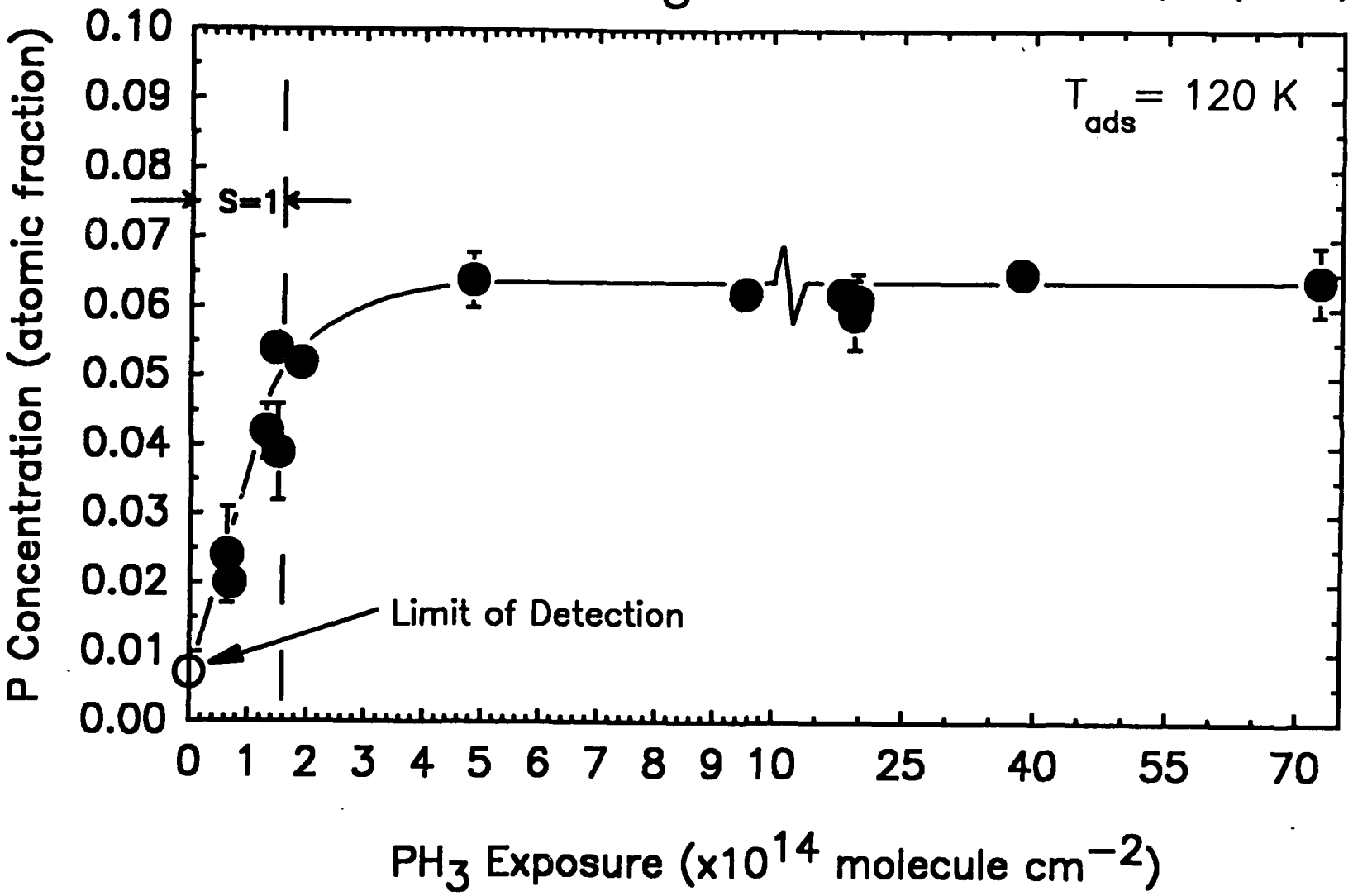

Taylor,
Wallace,
Choyke, Yates
Figure 5

Thermal Desorption from $PH_3/Si(111)-(7x7)$

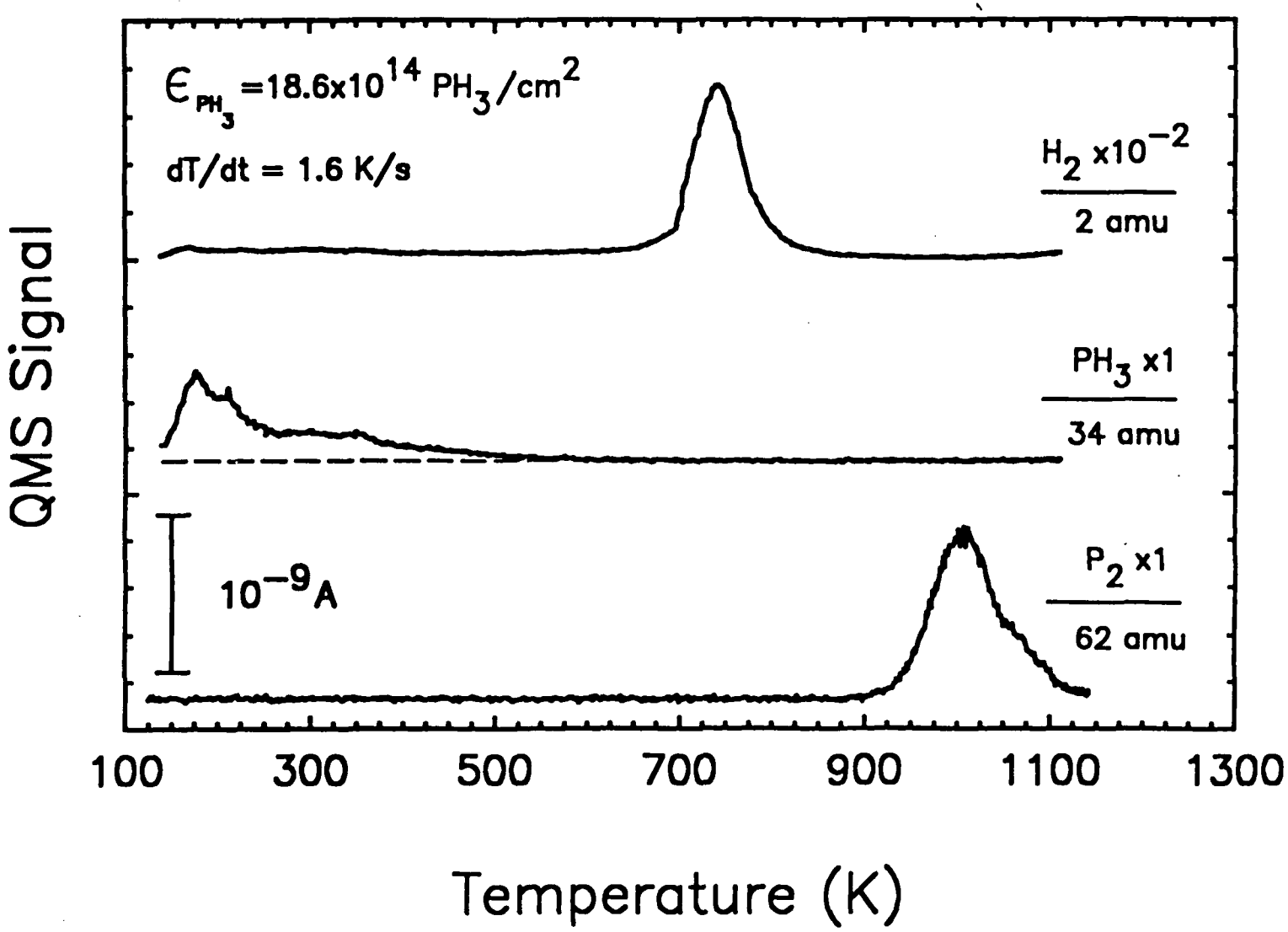

Taylor, Wallace, Choyke, Yate
Figure 6

Thermal Desorption of Molecularly Bound PH_3. Si(111)–(7x7)

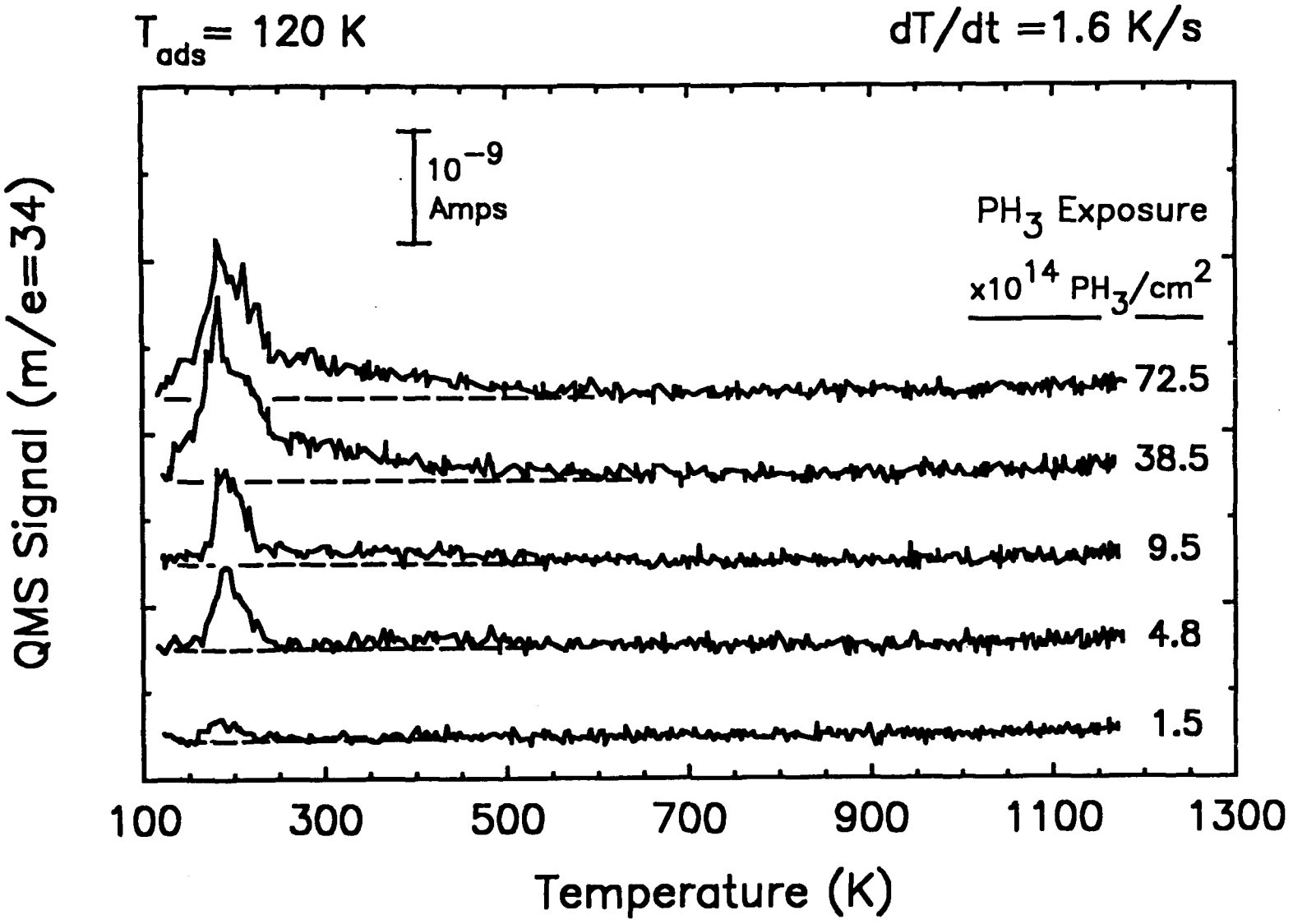

Taylor,
Wallace,
Choyke, Yates
Figure 7

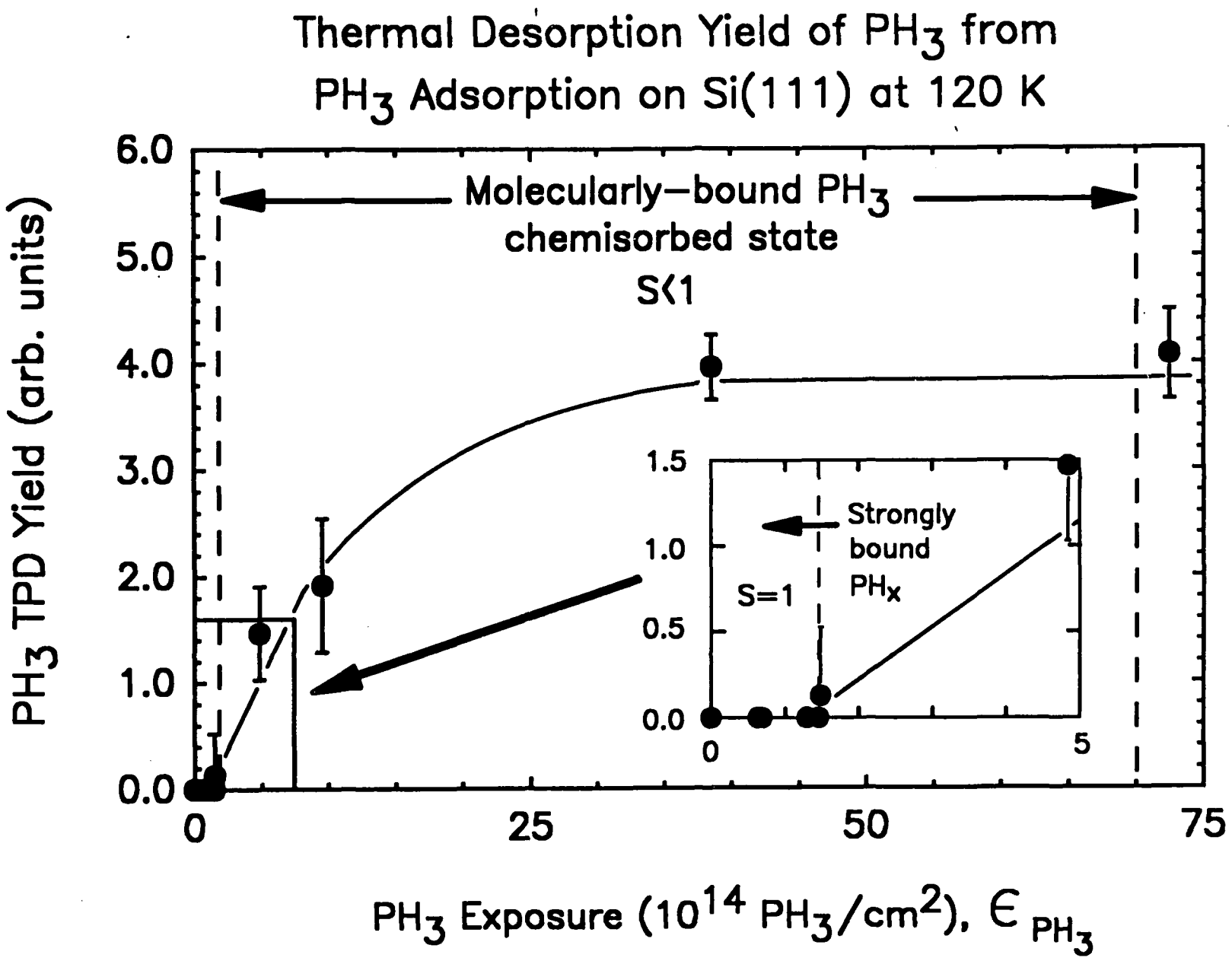

Taylor,
Wallace,
Choyke, Yat
Figure 8

Thermal Desorption of P_2 from PH_3. Si(111)–(7x7)

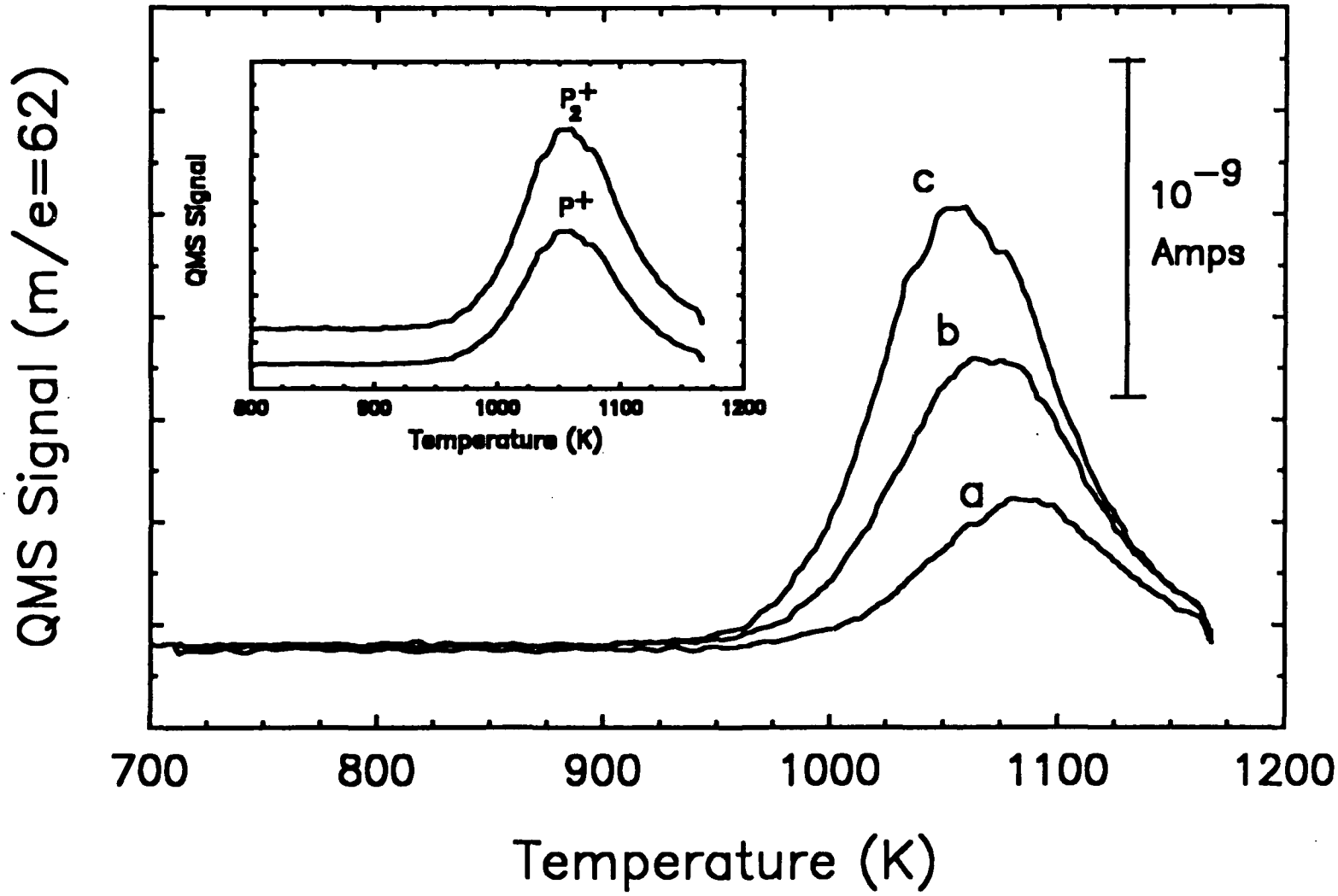

Taylor,
Wallace,
Choyke, Yates
Figure 9

Thermal Desorption of D_2 from D/Si(111)

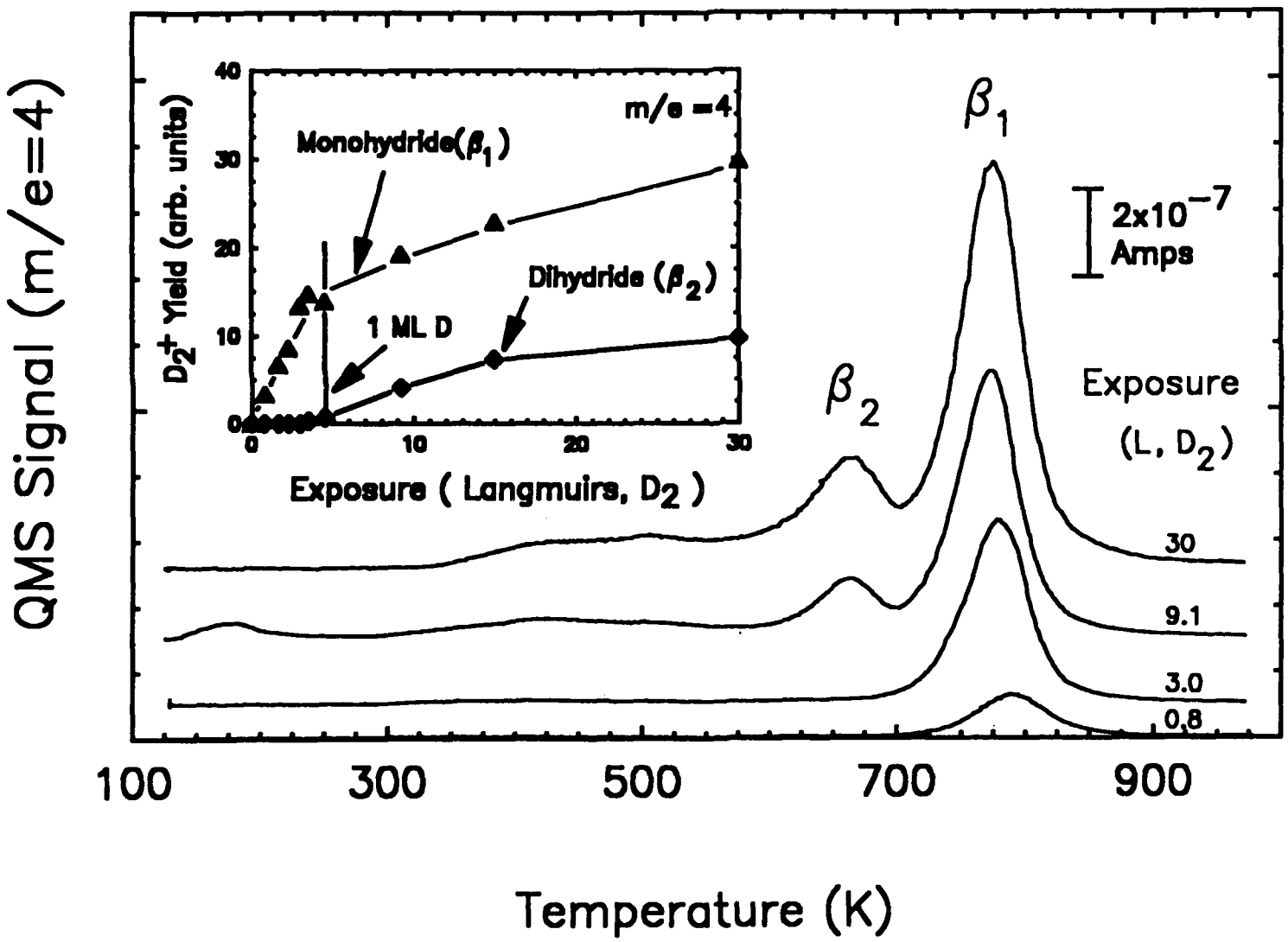

Taylor,
Wallace,
Choyke, Yate
Figure 10

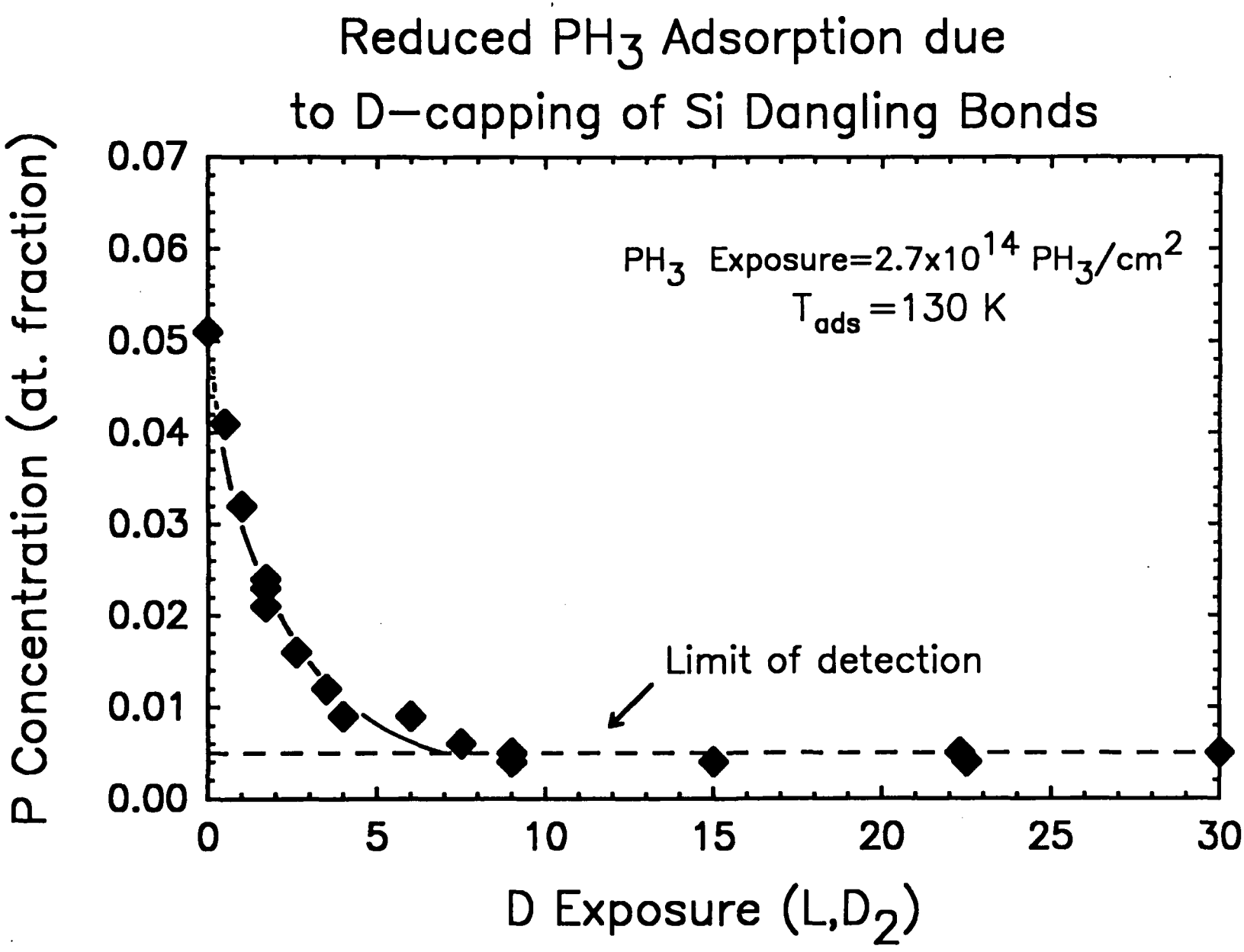

Taylor,
Wallace,
Choyke, Yate
Figure 11

Isotope Exchange Experiment for $PH_3/D/Si(111)-(7x7)$

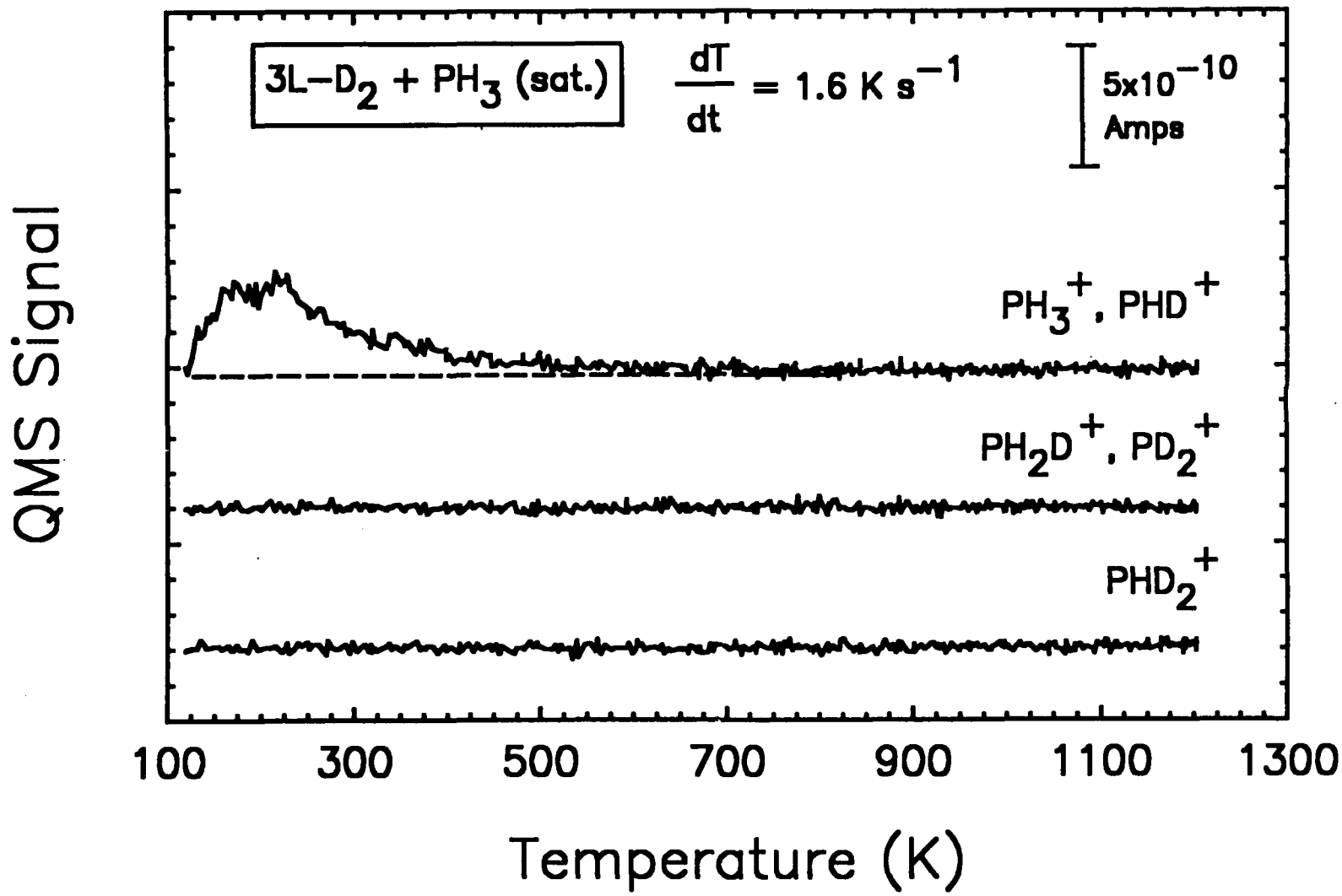

Taylor,
Wallace,
Choyke, Yate
Figure 12

Additional PH_3 Uptake on Saturated PH_3/Si(111) after Annealing to Different Temperatures

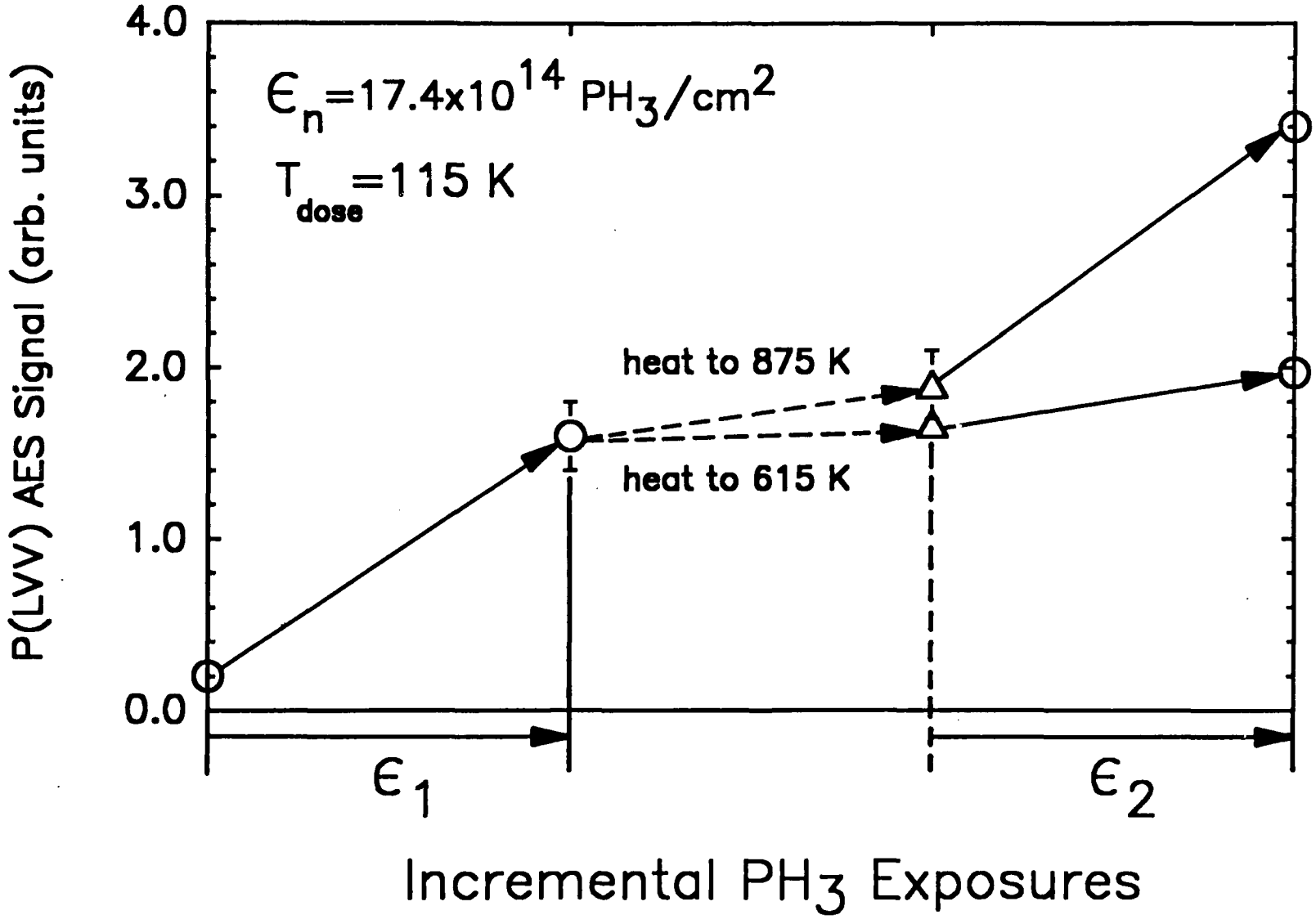

Taylor,
Wallace,
Choyke, Yat
Figure 13

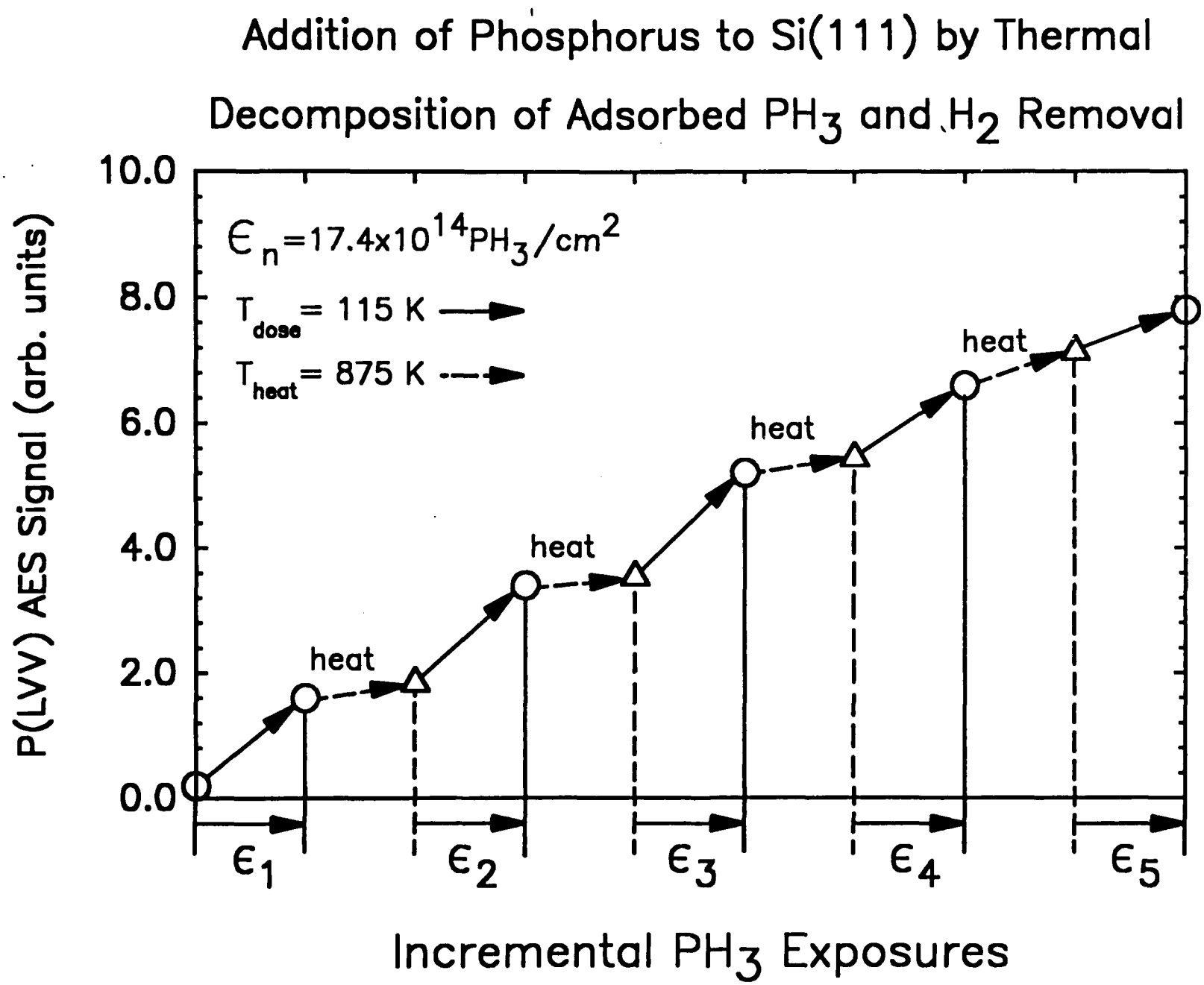

Taylor,
Wallace,
Choyke, Yate
Figure 14

The Reduction of the Si(LVV) AES Intensity by the Incremental Addition of Phosphorus from Decomposition of PH_3 on Si(111)

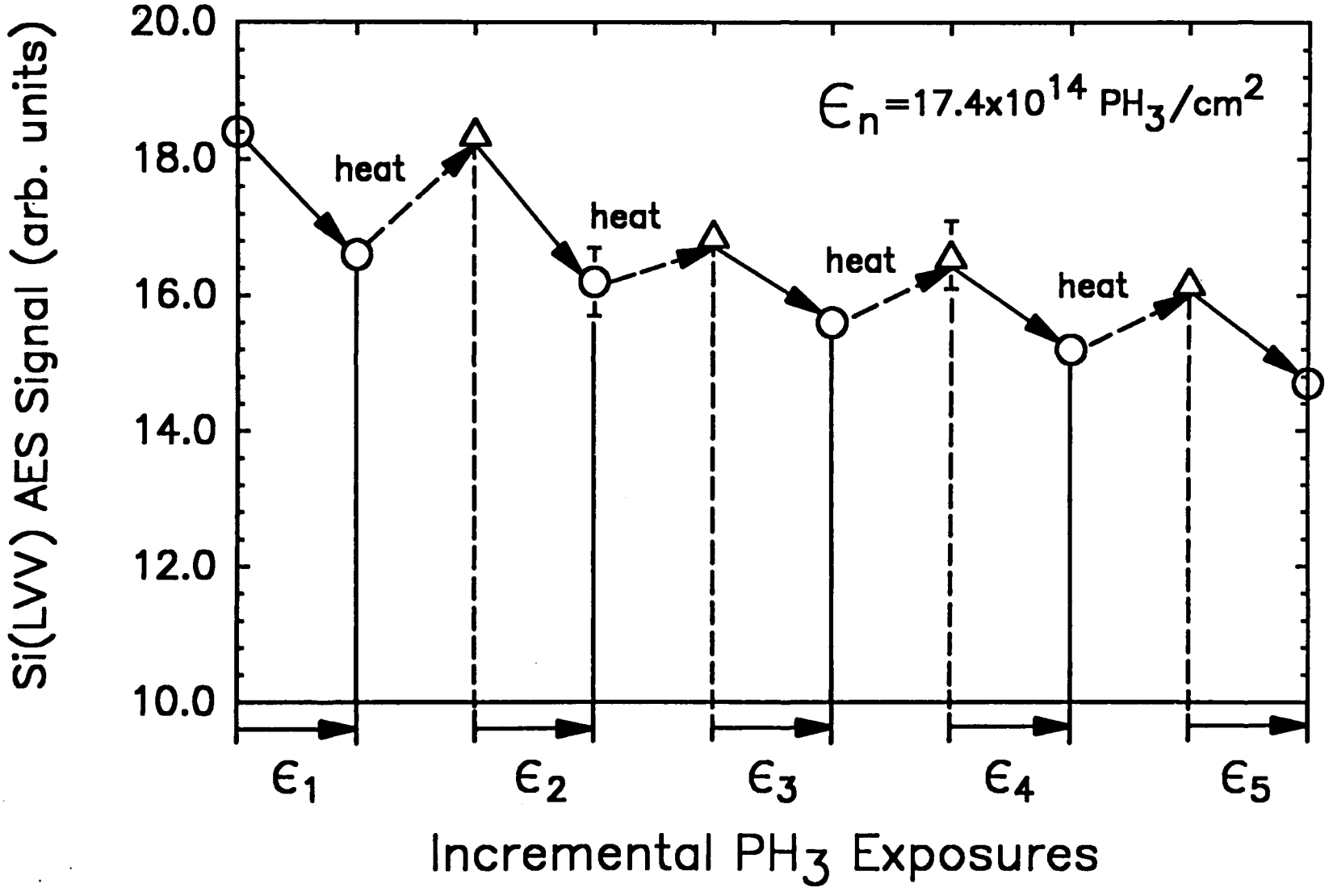

TECHNICAL REPORT DISTRIBUTION LIST - GENERAL

Office of Naval Research (2)
Chemistry Division, Code 1113
800 North Quincy Street
Arlington, Virginia 22217-5000

Commanding Officer (1)
Naval Weapons Support Center
Dr. Bernard E. Douda
Crane, Indiana 47522-5050

Dr. Richard W. Drisko (1)
Naval Civil Engineering Laboratory
Code L52
Port Hueneme, CA 93043

David Taylor Research Center (1)
Dr. Eugene C. Fischer
Annapolis, MD 21402-5067

Dr. James S. Murday (1)
Chemistry Division, Code 6100
Naval Research Laboratory
Washington, D.C. 20375-5000

Defense Technical Information Center (2)
Building 5, Cameron Station
Alexandria, VA 22314

Dr. Robert Green, Director (1)
Chemistry Division, Code 385
Naval Weapons Center
China Lake, CA 93555-6001

Chief of Naval Research (1)
Special Assistant for Marine Corps Matters
Code 00MC
800 North Quincy Street
Arlington, VA 22217-5000

Dr. Bernadette Eichinger (1)
Naval Ship Systems Engineering Station
Code 053
Philadelphia Naval Base
Philadelphia, PA 19112

Dr. Sachio Yamamoto (1)
Naval Ocean Systems Center
Code 52
San Diego, CA 92152-5000

Dr. Harold H. Singerman (1)
David Taylor Research Center
Code 283
Annapolis, MD 21402-5067

May 19 1990